

Structural features of the plane turbulent jet

J. N. Moum, J. G. Kawall, and J. F. Keffer

Department of Mechanical Engineering, University of Toronto, Toronto, Canada M5S 1A4
(Received 6 November 1978; final manuscript received 2 April 1979)

An experimental investigation of a two-dimensional turbulent jet in a quiescent environment has been carried out to determine the structural characteristics of the outer, intermittent turbulent motion. An overall picture of this motion was deduced from the results which indicate that, on the average, the turbulent bulges are of the same order of magnitude in the three coordinate directions and are tilted backward at an angle of approximately 26° with respect to the lateral axis but have no spanwise yaw. Furthermore, it was found that there is no periodicity associated with the motion and that no correlation exists between bulges on opposite sides of the jet center line.

I. INTRODUCTION

Although the plane turbulent jet has been the subject of considerable investigation over the past several years,¹⁻⁵ few data have been presented from which one can develop an overall understanding of the three-dimensional nature of the turbulence structure. This present work was undertaken in an attempt to fill this gap. The approach has been restricted to an examination of the most obvious features of the jet, viz., the outer, intermittent turbulent bulges or bursts, which are thought to be the primary agents in controlling the spread and growth of the flow. To this end, an analysis of various statistical quantities based on the turbulence indicator or intermittency function has been made.

In a previous investigation, Barsoum *et al.*⁶ examined the spanwise features of a two-dimensional wake using auto and space-time correlations of intermittency signals. From this, it was possible to deduce some of the gross characteristics of the turbulent bulges. The results showed that they were strongly three dimensional in nature and, on the average, had no spanwise yaw. Here, we use a similar statistical technique but extend the analysis so as to enable us to infer the overall three-dimensional configuration of the bulges, providing a first-order picture of the outer motion of the jet.

II. EXPERIMENTAL DETAILS

A definition sketch of the flow is shown in Fig. 1, where x is the streamwise coordinate, y is the lateral coordinate, and z is the spanwise coordinate. The jet was generated by a blower-type wind tunnel having appropriate flow-straightening elements, screens, and settling length, and a 12-1 contraction leading to a 305×53 mm nozzle. The exit velocity was 17.1 msec⁻¹ which resulted in a Reynolds number based on nozzle width of 5.9×10^4 . All measurements presented in this work were taken at $x/B = 10$, about $4B$ beyond the end of the potential core. Since the aspect ratio of the nozzle was rather small (approximately 6), side walls were used to insure that the central region of the flow was two dimensional at the above station.

Mean velocity, turbulence intensity, and shear stress data, obtained at $x/B = 10$, proved to be independent of z , for z within about $\pm 2.0B$, implying that the flow was reasonably two-dimensional over an adequately large

span. We note that Davies *et al.*,³ who used the same experimental facilities under similar test conditions, found the lateral distributions of the conventional mean and root-mean-square velocities, the intermittency factors, and the turbulent-zone-averaged mean velocities to be roughly self-preserving at $x/B = 10$.

Two conventional, normal hot-wire probes, designated as probes A and B, were used in conjunction with DISA 55 M01/55 M10 constant temperature anemometers to simultaneously measure streamwise velocity signals. These latter were used to determine the turbulence indicator functions. A traversing mechanism allowed each probe to be positioned to within ± 0.5 mm of any desired location. For spanwise space-time correlations, probe A was fixed in the half-intermittency region at $y_A = 1.81B$, $z_A = -0.595B$, $y = 1.81B$ being the line along which the intermittency factor was approximately 0.5, and probe B was placed at $y_B = 1.81B$, z_B , where $z_B = z_A + s_z$. For lateral correlations, probe A was fixed at $y_A = 1.81B$, $z_A = 0$ and probe B was located at y_B , $z_B = 0$, where $y_B = y_A \pm s_y$; or, the probes were positioned on opposite sides of the jet center line, in such a way that $z_A = z_B = 0$ and $y_B = -y_A$. Figure 2 illustrates the placement of the probes in the jet.

The anemometer signals were low-pass filtered at 5 kHz, recorded on magnetic tape by means of an Ampex PR2200 tape recorder and digitized with a PDP 11

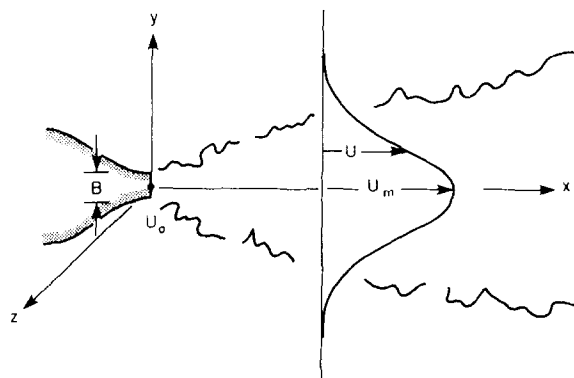


FIG. 1. Definition sketch. B = nozzle width, U_0 = exit velocity, U = local mean jet velocity, U_m = maximum mean jet velocity.

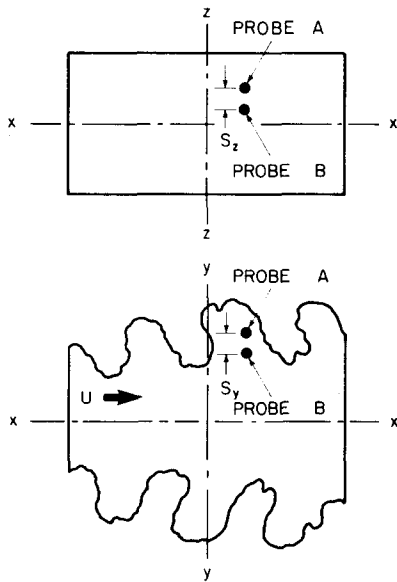


FIG. 2. Probe placement.

computer. The digital data were subsequently processed on an IBM 370-165 computer.

III. PROPERTIES OF THE FLOW

The turbulence indicator function, which is used to identify the turbulent/nonturbulent interface (or equivalently, the turbulent bulges) of an intermittently turbulent flow is defined as

$$I(t) = \begin{cases} 1 & \text{if turbulent fluid occurs at time } t, \\ 0 & \text{otherwise.} \end{cases}$$

In the present case, this function was generated by means of a digital technique, similar to the one described by Kawall and Keffer.⁷

The statistical properties which were examined are

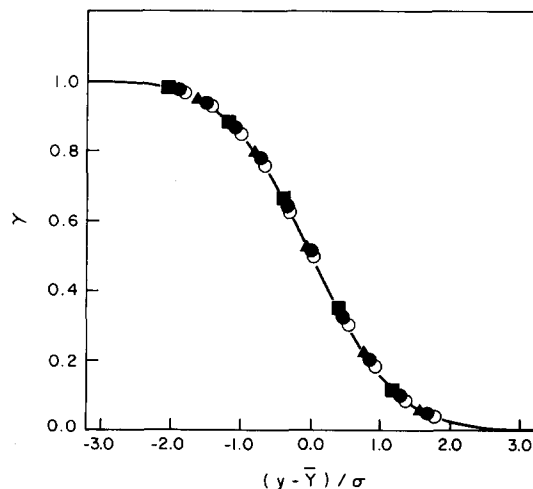


FIG. 3. Intermittency factor distribution. $y > 0$: ■, $z/B = -0.595$; ●, 0.0 ; ▲, $+0.595$. $y < 0$: ○, $z/B = 0.0$. —, Gaussian distribution function.

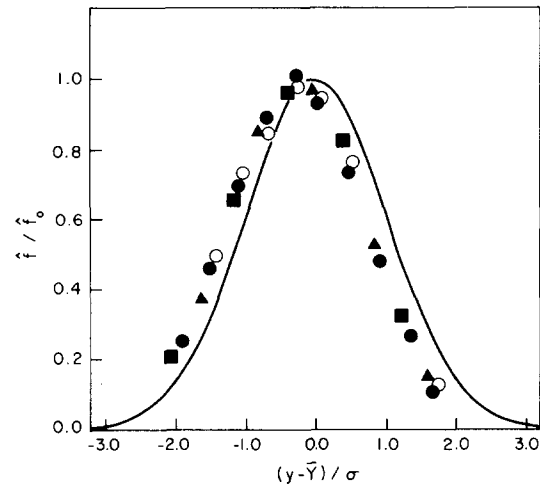


FIG. 4. Burst rate distribution. The symbols have the same meaning as in Fig. 3. —, Gaussian function.

(i) The intermittency factor γ which is the average value of the indicator function, i.e.,

$$\gamma = \bar{I} = \frac{1}{N} \sum_{i=1}^N I(t_i),$$

where N is the number of discrete values of $I(t_i)$ in a time period T , and $t_i = i(T/N) = i\Delta t$, $i = 0, 1, 2, \dots$

(ii) The burst rate, which is given by

$$\hat{f} = M/T,$$

where M is the number of turbulent (or potential) zones occurring at a given point during T .

(iii) The autocorrelation of the indicator function,

$$\rho_{II}(\tau) = \overline{\alpha(t)\alpha(t+\tau)} (\overline{\alpha^2})^{-1} \\ = \left(\lim_{T \rightarrow \infty} \frac{1}{T} \int_0^T \alpha(t)\alpha(t+\tau) dt \right) (\overline{\alpha^2})^{-1},$$

where $\alpha(t) = I(t) - \bar{I}$, τ is a time lag, and α^2 is the variance of $\alpha(t)$.

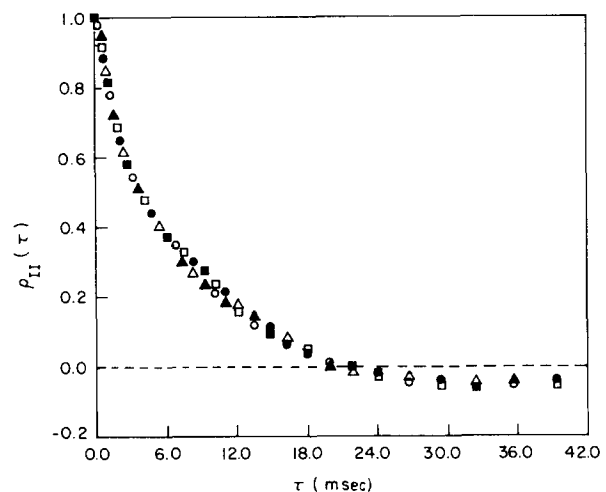


FIG. 5. Autocorrelation of the indicator function. ■, $z/B = -0.595$; ●, -0.314 ; ▲, -0.119 ; □, $+0.143$; ○, $+0.415$; △, $+0.691$.

(iv) The one-dimensional spectrum or autospectrum of the indicator function $E_{II}(n)$, which is the Fourier transform of $\overline{\alpha^2} \rho_{II}(\tau)$, i.e.,

$$E_{II}(n) = 2\overline{\alpha^2} \int_0^\infty \rho_{II}(\tau) \exp(-i2\pi n\tau) d\tau,$$

where n is a frequency such that $n \geq 0$.

(v) The space-time correlation of the indicator functions at two points, A and B, separated by a distance s ,

$$\rho_{IA'IB'}(\tau; s) = \overline{\alpha_A(\tau) \alpha_B(t+\tau)} / (\overline{\alpha_A^2} \overline{\alpha_B^2})^{1/2}.$$

With respect to (v), if A and B refer to the half-intermittency points on opposite sides of the jet center line, with coordinates (x, \bar{Y}, z) and $(x, -\bar{Y}, z)$, respectively, then the resulting space-time correlation (which we shall refer to as the interface correlation function) will tell us whether or not the interface motions on opposite sides of the jet center line are correlated. It is noted that Wygnanski and Gutmark⁸ examined this problem, using an interface correlation coefficient, $\rho_y^*(s_y)$, based on an intermittency function given by

$$I^*(t) = \begin{cases} +C & \text{if turbulent fluid occurs at time } t, \\ -C & \text{otherwise,} \end{cases}$$

where C is an arbitrary constant. It can be shown that

$$\rho_y^*(s_y) = 4\overline{I(y)I(-y)} - 4\overline{I(y)}^2 + 1,$$

where $s_y = 2y$ and $\overline{I(y)} = \overline{I(-y)}$. Clearly, for either fully turbulent regions or fully potential regions, $\rho_y^* = 1$. Moreover, if the interface correlation function is zero for $\tau = 0$, so that $\overline{I(\bar{Y})I(-\bar{Y})} = \overline{I(\bar{Y})}^2$, then $\rho_y^* = 0$.

IV. RESULTS AND DISCUSSION

Normalized intermittency factor distributions for various spanwise locations are presented in Fig. 3. As expected, the data follow the Gaussian distribution, i.e.,

$$\gamma(y) = \frac{1}{\sigma\sqrt{2\pi}} \int_y^\infty \exp[-(y' - \bar{Y})^2/2\sigma^2] dy',$$

where \bar{Y} can be considered to be the mean lateral position of the interface and σ is the standard deviation of the interface displacement about \bar{Y} .

Figure 4 shows the normalized burst rate profiles for the same spanwise locations. It is clear that there is no agreement between these profiles and the Gaussian model

$$\hat{f}(y) = \hat{f}_0 \exp[-(y - \bar{Y})^2/2\sigma^2],$$

where \hat{f}_0 is the maximum burst rate. We note that much the same thing has been found by Gutmark and Wygnanski⁵ for the plane turbulent jet and by Hedley and Keffer⁹ and by Kovaszny *et al.*¹⁰ for the turbulent boundary layer. On the other hand, the Gaussian burst rate model has been found by several workers (e.g., Refs. 11 and 12) to be quite suitable in the case of the two-dimensional turbulent wake. Kawall and Keffer⁷ have demonstrated that agreement between burst rate data for the wake and the model depends essentially on the technique used to generate the intermittency function. Thus, the lack of

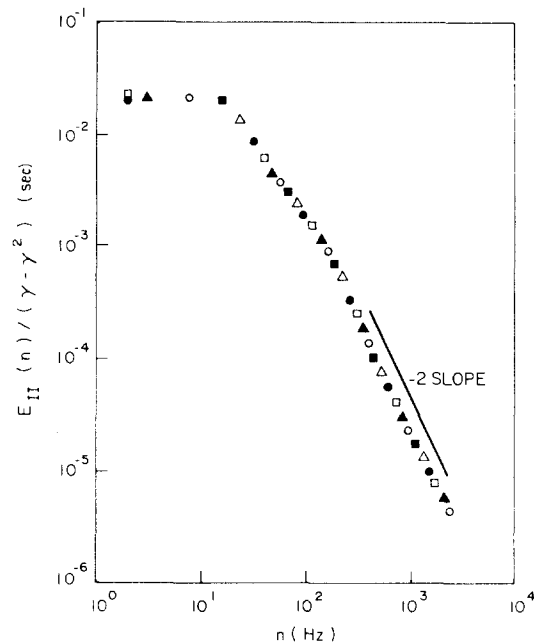


FIG. 6. Autospectrum of the indicator function. The symbols have the same meaning as in Fig. 5.

agreement in the present case may be a result of the insensitivity of our turbulent/nonturbulent discrimination procedure to turbulent and potential zone durations smaller than the Taylor microscale. This, however, is of little consequence as far as determination of the structure of the large-scale eddies is concerned.

It should be mentioned that the values of \bar{Y} , σ , and \hat{f}_0 were found to be independent of z , so that the collapse of the intermittency factor profiles and of the burst rate

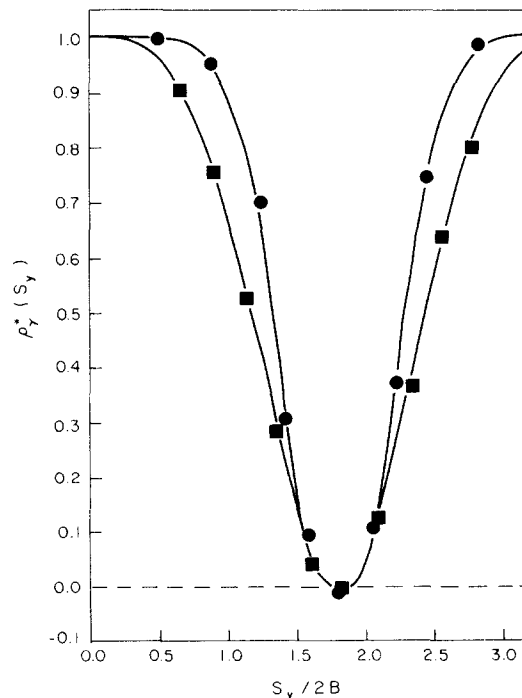


FIG. 7. Distribution of the interface correlation coefficient. ●, Wygnanski and Gutmark⁸; ■, present results.

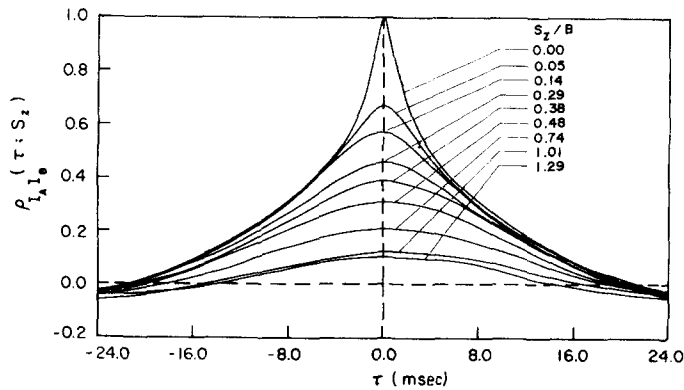


FIG. 8. Spanwise space-time correlation of indicator functions.

profiles substantiates that the flow was two dimensional.

Figures 5 and 6 show the autocorrelations and auto-spectra for various spanwise positions where $\gamma \approx 0.5$. These results are clearly independent of z , as expected. The absence of oscillations in the autocorrelations and of peaks in the spectra establishes that the interface motion is random in nature. The negative values of the autocorrelations at large time lags can be ascribed to the statistical instability which arises when signals of finite duration are Fourier transformed. (In the present case, the signal duration was 40 sec.) We note that the -2 slope displayed by the spectra is consistent with the view that the turbulence indicator function stems from a type of Poisson counting process.¹³

The distributions of the interface correlation coefficient, $\rho_y^*(s_y)$, obtained in the present study and by Wygnanski and Gutmark⁸ (for $x/B=10$) are presented in Fig. 7. It is clear that the two distributions have the same general shape, being symmetrical about the line $s_y = s_p$. The discrepancies between the two sets of data are probably a consequence of differences in the turbulent/nonturbulent discrimination procedures used to generate the intermittency functions. Our digital technique, unlike the analog technique employed by Wygnanski and Gutmark,⁸ incorporated both past and future turbulent/nonturbulent events. As well, the smoothing (or hold) times associated with the discrimination procedures may have been quite different. Neither of these factors

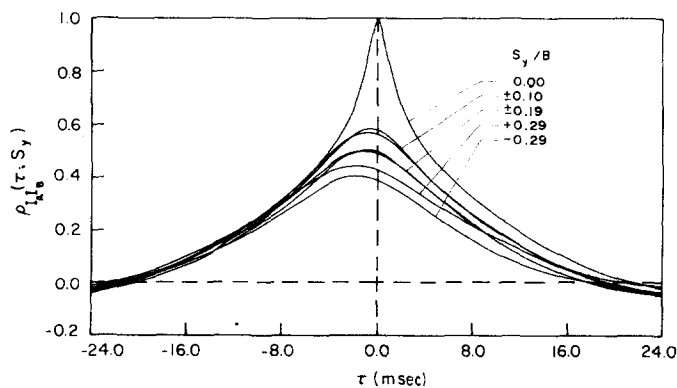


FIG. 9. Lateral space-time correlation of indicator functions.

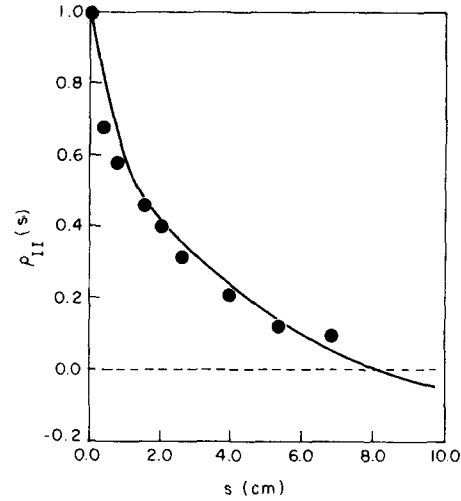


FIG. 10. Streamwise and spanwise autocorrelations of the indicator functions. —, $\rho_{II}(s_x)$; •, $\rho_{II}(s_z)$.

is likely to have significantly affected $\bar{I}(y)$, but either could have had a relatively large effect on $\bar{I}(y)\bar{I}(-y)$ and, hence, on $\rho_y^*(s_y)$.

Since ρ_y^* is essentially zero for $y = \bar{Y}$, one might conclude, as Wygnanski and Gutmark⁸ did, that the interface motions on opposite sides of the jet center line are statistically independent. We felt that such a conclusion required further justification, inasmuch as the interface motions could be significantly correlated for nonzero lag times. Accordingly, we determined the interface correlation function, $\rho_{I_{AIB}}(\tau; s_p)$. This was found to be zero for all τ , thus establishing the validity of the conclusion given here. It is interesting to note that the interface model proposed by Townsend¹⁴ is consistent with this conclusion, although it predicts that the bulges would occur in a periodic fashion on each side of the jet center line.

The spanwise space-time correlation of the indicator functions, $\rho_{I_{AIB}}(\tau; s_z)$, is plotted for several values of s_z in Fig. 8. It can be seen that the various curves are essentially symmetrical and peak at $\tau=0$ with the maximum correlation values decreasing monotonically as s_z increases. Evidently, the turbulent bulges (because they are of limited lateral extent) are three dimensional in nature, and, on the average, have no spanwise yaw, i.e., their contour lines form symmetrical figures (in the $x-z$ plane).

Figure 9 shows the lateral space-time correlations, $\rho_{I_{AIB}}(\tau; -s_y)$ and $\rho_{I_{BIA}}(\tau; +s_y)$. Except for the fact that the maximum correlation values decrease as s_y increases, these curves are clearly different from those shown in Fig. 8, for nonzero separations, being noticeably asymmetrical and peaking at time lags which become progressively more negative as s_y increases. It should be noted that for s_y less than about $0.2B$, $\rho_{I_{AIB}}(\tau; -s_y) \approx \rho_{I_{BIA}}(\tau; +s_y)$. The interpretation here is that the bulges are, on the average, tilted backward with respect to the y axis.

Following LaRue and Libby,¹⁵ we invoke Taylor's hy-

pothesis, viz., $s_x = U_c \tau$, where U_c is an appropriate convection velocity, and define the tilt angle as $\tan^{-1} |d(U_c \tau_p)/ds_y|$, where τ_p is the time lag at which $\rho_{IAIB}(\tau; s_y)$ peaks. In the first of two calculations based on this definition, U_c was assumed constant and equal to the mean jet velocity at the half-intermittency point. This yielded a tilt angle of 25° . In the second computation, U_c was allowed to vary with s_y and this produced an average angle of 26° .

A first-order estimate of the ratio of the characteristic spanwise extent of the bulges, L_z , to their characteristic streamwise extent, L_x , can be obtained from a comparison between $\rho_{II}(s_z)$ and $\rho_{II}(s_x)$ (Ref. 6). Figure 10 shows the variation of the peaks of the spanwise space-time correlation curves (Fig. 8) with s_z , which represents $\rho_{II}(s_z)$, together with a plot of $\rho_{II}(s_x)$, which was determined from $\rho_{II}(\tau)$ (Fig. 5) by means of the Taylor hypothesis. These results clearly imply that L_z/L_x is approximately equal to unity.

Choosing σ as a measure of the characteristic lateral extent of the bulges, L_y , and $U_c/2\hat{f}_0$ as a measure of L_x , (Ref. 6 and 16) we found L_y/L_x to be about 0.8. We note that this value is roughly $3\frac{1}{2}$ times larger than the estimate based on the γ and \hat{f} measurements of Bradbury,¹ reported by Townsend.¹⁴ In contrast, the present value for L_y/\bar{Y} , which is 0.33, is only about 30% larger than Bradbury's.¹⁴ This suggests that the major source of the discrepancy between the estimates of L_y/L_x is the \hat{f}_0 value used in the calculation of L_x , since the error associated with the measurement of σ/\bar{Y} is not likely to exceed about 20% (Ref. 7). Bradbury¹ stated that the "experiment" which he carried out to measure \hat{f} was "extremely crude" and that the resulting data may have been as much as 50% in error. On the basis of visual comparisons between the intermittent velocity signals and the corresponding turbulence indicator functions, we concluded that our \hat{f}_0 value could not be more than 20% in error. Accordingly, the present estimate of L_y/L_x is considered to be reasonably accurate.

V. SUMMARY AND CONCLUDING REMARKS

The results obtained in this study have shown that the intermittent large-scale eddies of the two-dimensional

jet arise essentially randomly and independently on opposite sides of the jet center line. On the average, these bulges have roughly the same dimensions in the three coordinate directions and are tilted backward at an angle of about 26° to the lateral axis but have no spanwise yaw. The tilt is as would be expected from the physics of the flow: pockets of high-speed turbulent fluid are ejected from the central core of the jet and are retarded by the contiguous potential fluid.

From the present findings and those of Barsoum *et al.*⁶ and LaRue and Libby,¹⁵ it is evident that the plane jet and plane wake have different interface topographies, the bulges of the latter flow being elongated in the streamwise direction⁶ and tilted forward at an angle of about 31° to the lateral axis.¹⁵ This lends support to the view that entrainment rate depends on bulge configuration, as the observed entrainment constant for the wake is significantly greater than that for the jet.¹⁴

ACKNOWLEDGMENT

This research was sponsored by the National Research Council of Canada under Grant Number A-2746.

¹L. J. S. Bradbury, *J. Fluid Mech.* **23**, 31 (1965).

²G. Heskestad, *J. Appl. Mech.* **32**, 721 (1965).

³A. E. Davies, J. F. Keffer, and W. D. Baines, *Phys. Fluids* **18**, 770 (1975).

⁴P. E. Jenkins and V. W. Goldschmidt, *Phys. Fluids* **19**, 613 (1976).

⁵E. Gutmark and I. Wygnanski, *J. Fluid Mech.* **73**, 465 (1976).

⁶M. L. Barsoum, J. G. Kawall, and J. F. Keffer, *Phys. Fluids* **21**, 157 (1978).

⁷J. G. Kawall and J. F. Keffer (to be published).

⁸I. Wygnanski and E. Gutmark, *Phys. Fluids* **14**, 1309 (1971).

⁹T. B. Hedley and J. F. Keffer, *J. Fluid Mech.* **64**, 645 (1974).

¹⁰L. S. G. Kovasznay, V. Kibens, and R. F. Blackwelder, *J. Fluid Mech.* **41**, 283 (1970).

¹¹J. G. Kawall and J. F. Keffer, *Phys. Fluids* **22**, 31 (1979).

¹²J. C. LaRue and P. A. Libby, *Phys. Fluids* **19**, 1864 (1976).

¹³J. G. Kawall and J. F. Keffer, in *Structure and Mechanisms of Turbulence II*, edited by H. Fiedler (Springer-Verlag, Berlin, 1978) p. 85.

¹⁴A. A. Townsend, *J. Fluid Mech.* **26**, 689 (1966).

¹⁵J. C. LaRue and P. A. Libby, *Phys. Fluids* **17**, 873 (1974).

¹⁶S. Corrsin and A. L. Kistler, NACA Report 1244 (1955).